Classification of Photo-Acoustic Emission in Direct Laser Interference Pattering for Identifying the Spatial Period

Tobias Steege*[1], Adrian Belkin[1], Christoph Zwahr[1], and Andrés F. Lasagni[1,2]

[1]*Fraunhofer Institute for Material and Beam Technology IWS, Winterbergstr. 28, 01277 Dresden, Germany*
[2]*Technische Universität Dresden, Institut für Fertigungstechnik, George-Bähr-Str. 3c, 01069, Germany*
**Corresponding author's e-mail: tobias.steege@iws.fraunhofer.de*

Direct Laser Interference Patterning (DLIP) is a versatile tool used to produce microstructures for functionalized surfaces on different materials. However, monitoring strategies are needed to ensure repeatability and quality control during the fabrication of surface patterns with micro- and submicron resolution features. This study proposes a new approach for identifying the spatial period on the surface using airborne acoustic emission during DLIP. The acoustic emission parameters from a single laser pulse on the material are analyzed using different prediction algorithms to classify and compare different spatial periods. Line-like patterns were produced on aluminum substrates using a pulsed laser source, and the laser fluence was varied to obtain variation in the data set. The preliminary results show that the four algorithms can detect and identify the spatial period for different laser fluences with an accuracy of up to 96%. This approach could be used for an automated setup workflow and eliminates the need for manual measurement of this parameter. It is an important step towards a fully automated initialization of surface processing in the micrometer range.
DOI: 10.2961/jlmn.2024.01.2005
Keywords: Direct Laser Interference Patterning (DLIP), microstructures, functionalized surfaces, monitoring strategies, acoustic emission, prediction algorithms

1. Introduction

Today, significant opportunities for material processing can be achieved by laser technology, particularly in the domain of surface modification. The enhancement of various material properties is enabled by the ability to control the surface topography precisely, leading to the incorporation of the materials into a wide range of products and devices. By manipulation surface topography, for example, the hydrophobic properties of a surface can be influenced. This leads to the creation of self-cleaning surfaces, where dust and dirt particles are carried away by rolling water droplets [1]. Conversely, surfaces can be made more adhesive for specific applications, such as medical implants [2] where integration with tissue is required.

Furthermore, traditional methods in areas like cutting, drilling, and welding are increasingly being replaced by laser technology due to its precision and versatility [3,4]. In the field of surface microfabrication, numerous techniques based on lasers, including Direct Laser Writing (DLW) [1], Laser-Induced Periodic Surface Structures (LIPSS) [5], and Direct Laser Interference Patterning (DLIP) [6], are employed.

DLIP, in particular, is an advanced technology that allows for the creation of periodic micro- and nanoscale structures on material surfaces. This method utilizes the generation of an interference pattern in a single laser spot by superimposing two or more coherent laser beams from a one laser source. A wide range of periodic patterns can be created by using different wavelength and or adjusting polarization of the laser light, as well as the number of beams and the angles at which they intersect [7,8]. It has already been applied successfully to a variety of materials, including metals [9], ceramics [10], and glass [11].

The determination of specific properties for a material, such as hydrophobicity [1], light reflection [12] or friction characteristics [13], is influenced by the spatial period, which is the distance between successive peaks in the periodic structure. The importance of the precise knowledge of this process parameter has a direct influence of the resulting surface structures.

To determine process parameters such as the beam diameter or the working position, different methods are available today. For well-established laser processes as laser drilling and welding the capture of process lighting with CCD and CMOS cameras, or the airborne sound and contact microphones for recoding the process noise are established [14]. For laser texturing processes, for example DLW, the analysis of laser beam information such as plasma propagation has been successfully used for finding the focal position. Furthermore, methods for evaluating the airborne or structure-borne acoustic emission (AE) during laser micromachining are also being used for process monitoring [14,15]. For instance, studies on femtosecond laser interactions with silicon carbide employed AE techniques for a detailed understanding of the process dynamics. Similarly, AE monitoring has been successfully used in combination with high-speed cameras to study rust removal by pulsed lasers. For surface texturing, Evgueni et al. [16] showed that the surface-acoustic emissions in copper foils can be recorded with a contact microphone and relevant process information such as the change in pulse energy can be detected. However, the results show that the surface processing based on AE information alone is still challenging due to the complex non-linear ablation processes and the underlying time-varying statistical and spectral AE signatures. In a later work, a correlation between focus change and AE was shown [16]. In addition, Schulze et al. [17] demonstrated and auto-focusing approach for laser processing with picosecond pulses on the basis of the audio signal, whereby an additional visual evaluation with a CCD camera was used for higher accuracy. Advanced solutions based on real-time multi-sensor systems are already available for quality monitoring, e.g. the detection of the surface roughness. Additionally, it has been shown that AE could be used to determine the ideal working position as well as the spot diameter for DLIP [18]. However, a comprehensive analysis regarding the propagation of the interference volume, coupled with the evaluation of the resulting spot diameter on the material at the working position, has not been conducted thus far. In addition, measurements at different positions (acoustic sweep) are requited for both methods.

This work presents the first approach to predict the spatial period from the AE of the process by utilizing different classification algorithms by measurement at the working position. In particular, it focuses on the analytical evaluation of single laser pulses and the applicability of this parameter for the prediction, as well as comparing different prediction algorithm.

2. Materials and Methods

2.1 Materials

In this study, aluminum has been selected as reference material due to its wide range of applications, such as in the medical applications and aerospace [19] sector. The aluminum samples were unpolished, leading to a surface roughness of approximately 98 nm, as measured according to the DIN-ISO 25178 standards. Prior the laser treatment, all samples were cleaned of any contaminations using ethanol. After laser processing, the samples were not subjected to any further cleaning procedure.

2.2 Experimental setup

Figure 1 shows the used experimental setup, which includes the Direct Laser Interference Patterning (DLIP) technique

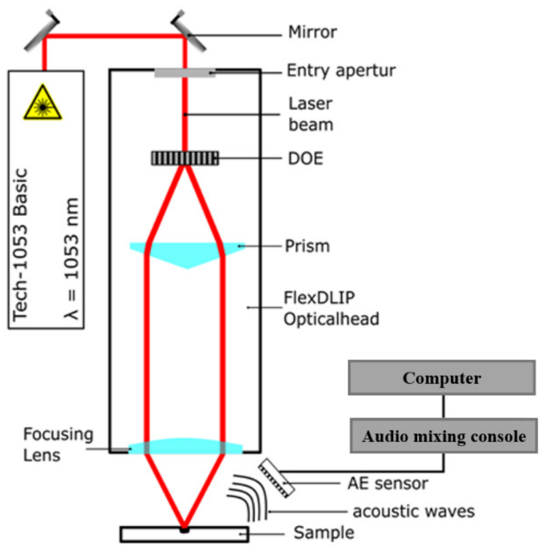

Fig. 1 Schematics of the employed experimental set-up showing the two-beam DLIP configuration as well as the AE sensor.

complemented by acoustic process measurement. The DLIP experiments involves the use of a coherent laser beam, which is divided into two sub-beams by a diffractive optical element. The angle of the sub-beams can be changed by adjusting the prism and the focusing lens distance, thus enabling control over the spatial period of the interference. For a two-beam configuration as used in this experiments, the result is a line-like periodic texture and the spatial period Λ can be obtained by:

$$\Lambda = \frac{\lambda}{2\sin\alpha}$$

where λ is the wavelength of the laser and α is the included angle between the individual laser beams.

The sub-beams intersect approximately 3.6 mm above the focal plane of the focusing lens (40mm), which allows improved control of surface topography by increasing the processed area and thus reducing peak laser fluences. This has also the advantage to increase the available size of the interference volume as well as reducing the variation of the spatial period. The used laser source was a Q-switched Nd:YLF laser (Laser export Tech-1053 Basic, Moscow, Russia) with a wavelength of 1053 nm generating 12 ns pulses with pulse energies up to 290 µJ (at 1 kHz). The laser power was not varied in these experiments, as this would have the same effect as changing the distance to the microphone.

In the setup, the free-field microphone M30 (Earthworks Audio, Milford, USA) was positioned diagonally above the laser interaction zone, at distance of 50 mm and an oriented angle of 25°, ensuring both beams were symmetrically oriented to the sensor. While the precise positioning of the microphone is critical to ensure optimal audio capture, the distance and angle of the sensor only affect the amplitude of the recorded signal and not the characteristic features or the frequency content of the signal itself. The microphone was connected to a computer using an audio mixing console AG06 (Yamaha, Hamamatsu, Japan). Characterized by an omnidirectional measurement capability, the microphone has a frequency bandwidth spanning from 3 Hz to 30 kHz and a sensitivity of 34 mV/Pa. The continuous audio signal was captured with a frequency of 96 kHz, in line with the maximum frequency of interest. Both the amplitude and time response of the signal were recorded.

The AE signal of 10x10 mm laser fields was recorded, while moving high precision motorized axes (Aerotech, PRO165LM, Pittsburgh, USA) at 3 mm/s perpendicular to the beams, so that 100 µm spacing between each individual laser pulse was achieved to avoid undesired overlapping. The emission for the spatial periods of 4.0 µm, 6.0 µm and 8.0 µm, by varying the interference angles between 31.7° and 7.1° at the working position was recorded.

2.3 Signal Parameters for acoustic emission

The qualitative analysis of acoustic emission is typically employed in structural or material-based acoustic emission testing, where sensors are directly attached to the material being tested [20,21]. In this context, the signals represent characteristic quantities, and their statistical distribution is examined over the observation duration to abstract a transient waveform of an AE signal into relevant and significant key indices. Figure 2 shows the AE parameters that are most commonly used[22].

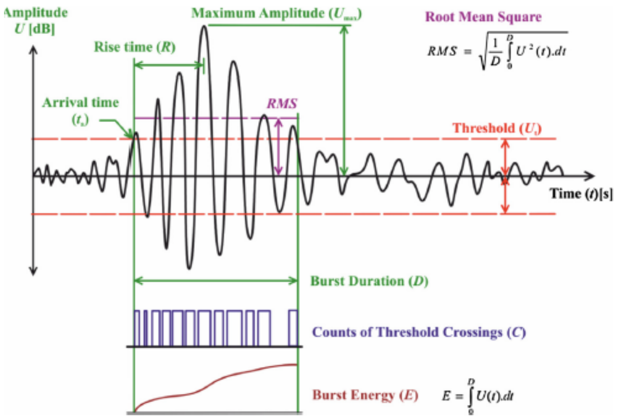

Fig. 2 Acoustic emission parameters for a single event.

All parameters can also be applied to single pulse laser ablation as a similar waveform is recorded. When the distance between the recording sensor and the emission source remains fixed, as in process monitoring, the arrival time is not of interest and the synchronization of the laser trigger signal with the recording can be neglected. Thus, onset detection algorithms[23] can be used to identify single laser pulses in a recording. The magnitude of the AE signal, indicated by the maximum amplitude, provides information about the energy released during the laser pulse. The rise time, which represents the time taken by the signal to rise to its peak, can offer insights into the speed of the event, as well as the duration until the signal falls below the noise level. The duration of the signal can also be determined by counting the threshold crossings and calculating the signal energy. Both parameters can be used to obtain information about the activity level and distribution of the laser pulse.

3. Results and Discussion

3.1 Analysis of the Dataset and feature construction

A discrete Fast Fourier Transformation (FFT) was performed to analyses each of the audio samples as well as to identify noise of the machine [24]. A Butterworth band-pass filter was applied, since only the frequency range from 18 kHz to 22 kHz is required for the calculation, as already reported [18]. Appling an onset detection algorithm, utilizing threshold filter each single laser pulse was extracted. Figure 2 shows the median sound profile of eight laser spots with a spatial period of 8 µm and laser power of 255 mJ. As can be seen, the length of the ablation signal is less than 1 ns, in contrast to the pulse length of the used laser source (12 ns). Indicating, that the recorded signal is the shockwave resulting from the laser-material interaction. This observation suggests that material removal and the generation of a plasma plume primarily occur within the initial moments of the irradiation event. The 1 ns duration of the sound wave is generated when the absorption length of the material is surpassed, leading to the occurrence of a laser-supported detonation (LSD). Further analysis of the underlying effect and a detailed investigation of the shockwave propagation velocity and its characteristics can be found elsewhere [25,26]. From each pulse the qualitative AE parameters were extracted and shown as a pairwise relationships in Figure 4. The diagonal plots display distribution of a single variables, while the other show the correlations between pairs of variables. As it can be observed, the maximum amplitude can be seen as similar for the different spatial periods. The same effects can be observed for the Burst Energy and the RMS of the signal. Which can be attributed to the same effect, as for the calculation of this parameters the maximum amplitude has a larger influence (see Figure 2). The variation for this parameter can also be attributed to two different effects that must be considered when changing the spatial period. When two laser beams are overlapped under a certain angle, an elliptical laser spot is produced, which can clearly be seen for smaller angles (e.g. spatial period of 4 µm) [27]. Thus, when the spatial period is changed from 8 to 4 µm, the size of the laser spot increases by approximately 10 % for the used experimental setup [28]. Therefore, larger amounts of material can be ablated due to the increased laser spot area, resulting in higher maximum amplitudes of the AE. However, it is known that for DLIP with ns pulses, the temperature at the maximum positions, under constant energy density, decreases as the spatial periods decrease. This phenomenon can be attributed to the increasing heat coefficient between interference maxima and minima, which leads to enhanced heat diffusion into the interference minima positions [29]. In consequence, the amount of ablated material can decrease and therefore also the maximum amplitudes.

Interestingly, the Rising Time for the different spatial periods is nearly identical, suggesting that there is no different in the shockwave generation. Due to the large overlaps for the AE parameters for each spatial period, it can be derived that for each of the spatial period, it can be inferred that no parameter can be used on its own for determination. Showing that the qualitative analysis of the AE parameters utilizes no immediately additional information if only recording at the working position is analyzed. It was shown, that the maximum amplitude of the signal directly corresponds with a variation of the working position.

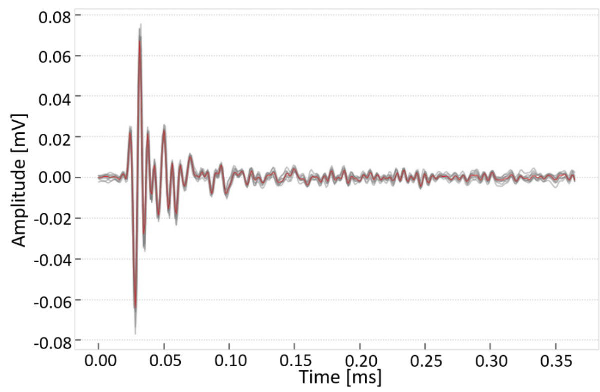

Fig. 3 Median sound profile of eight laser spots on alluminum steel for a spatial period of 8 µm and pulse energy of 255 mJ.

3.2 Prediction approach and validation

Four different algorithms were chosen to predict the spatial period from the extracted AE parameters of the recorded

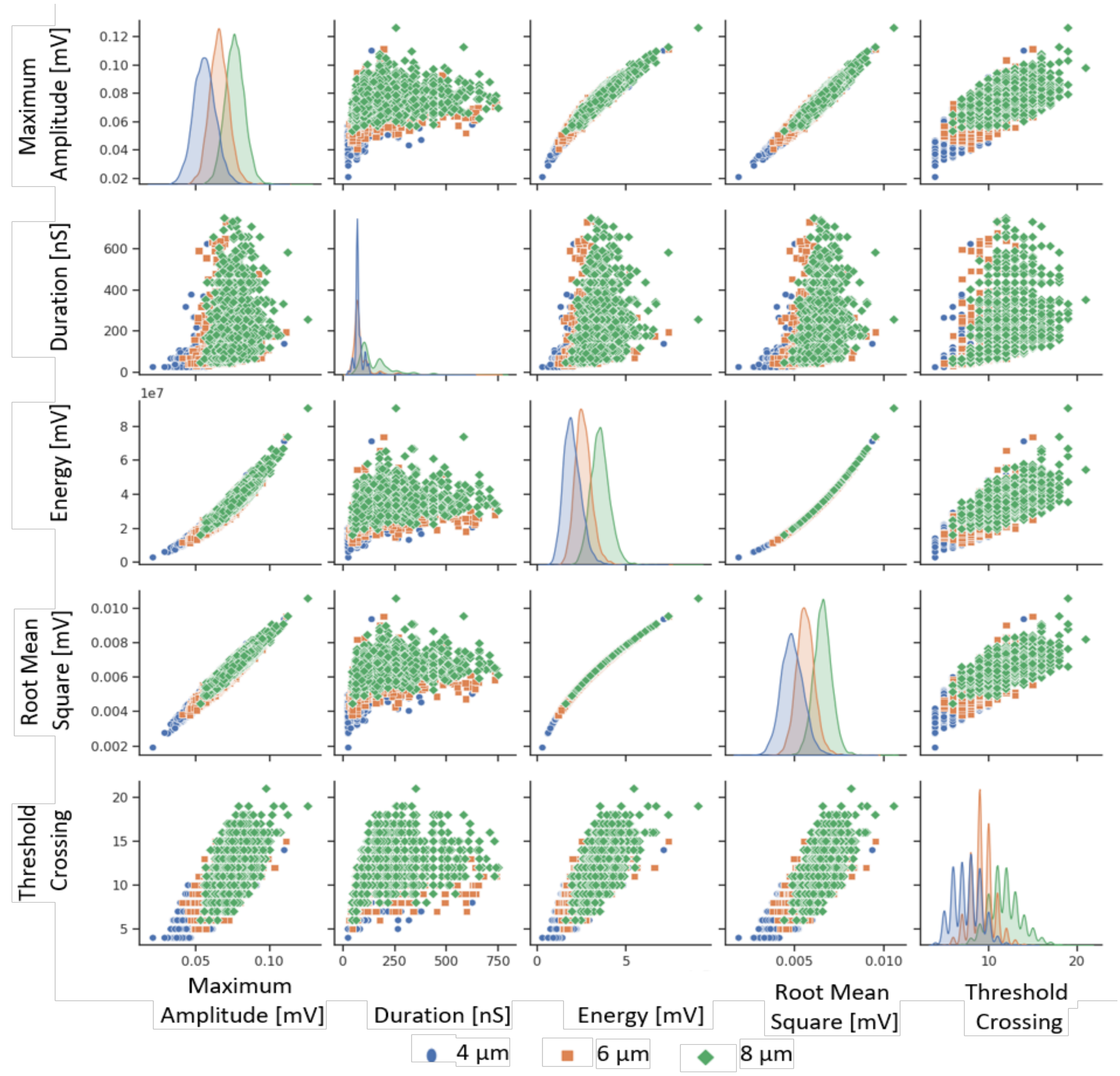

Fig. 4 Qualitative AE parameters of single laser pulse ablation on aluminum for three different spatial periods, 8 um, 6 um and 4 um for pulse energy of 255 mJ.

data. The dataset was split into 80% for training and 20% for validation, and each set of AE parameters was used as input. A total of 30,000 parameter sets were used for the training, with 10,000 single laser pulses for each spatial period. The target values (class labels) were defined as the three spatial periods, 8 µm, 6 µm and 4 µm. For the algorithms, a Support Vector Machine (SVM) was used, as this approach can handle high-dimensional data and is useful when the data is not linearly separable. A linear kernel function was used, because the input parameters do not need to be normalized. K-nearest neighbors (KNN) was selected as a non-parametric method, classifying data based on the majority class of their k nearest neighbors. Furthermore, Random Forest (RF) was chosen, because it combines uncorrelated decision trees, where each tree depends on the values of a random vector. Additionally, a neural network approach (NN) using a Multi-layer Perceptron was used, capable of representing non-linear connections between the parameters. For the RF and NN models, a grid search was performed to determine the optimal parameters. A Bayesian optimization technique was utilized to shorten the computing[30]. Figure 5 illustrates the comparison of prediction accuracy among the algorithms, revealing that all four algorithms are capable of predicting the spatial period with an accuracy exceeding 75%. Notably, the Random Forest (RF) approach demonstrates the highest accuracy at 96% due to its utilization of multiple decision trees, which effectively reduces variance. The results affirm that trained algorithms can effectively determine the spatial period prior to texturing through the use of AE measurements.

This approach proves highly valuable when integrated with an AE-based autofocus system for automated machine setup, as changes in the spatial period can occur when altering the distance between optical elements (such as adjusting the focusing lens).

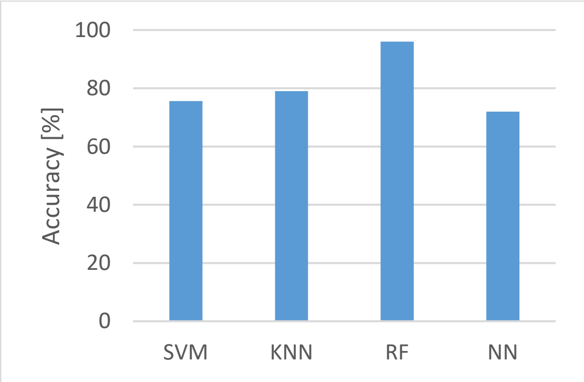

Fig. 5 Comparison of the accuracy of different algorithms to predict the spatial period.

4. Conclusions

In this work, qualitative AE parameters were applied to analyze the Acoustic Emission (AE) generated by single-pulse ablation on aluminum using Direct Laser Interference Patterning (DLIP). As a first objective, the response of the acoustic transducer of the ablation events was investigated and AE parameters, including Maximum Amplitude, Rise Time, and Burst Energy were calculated. It was observed that no direct correlation exists between a single AE parameter and the resulting spatial period of the structure. Therefore, four different classification algorithms were applied to the dataset. The result demonstrated shows that in by combination combining multiple of the AE parameters, the spatial period can be determined. Notably, the Random Forest approach achieved an accuracy of 96%, indicating its potential for monitoring the spatial period in industrial applications.

In future research, our focus will extend to studying the AE parameters induced by various types of lasers, aiming to enhance our understanding of acoustic emission effects. Additionally, we plan to gather more data for classification purposes by investigating the frequency response of the laser pulses. These endeavors will contribute to a deeper comprehension of the AE phenomenon and enable more accurate classification and prediction models.

Acknowledgments and Appendixes

This work was funded partial from the European Union under grant agreement no. 101091514 and the German Federal Ministry of Education and Research (BMBF) within the framework concept „Zukunft der Wertschöpfung – Forschung zu Produktion, Dienstleistung und Arbeit“ (funding code 02P20A050 – 02P20A057). The work of A.L. was supported by the German Research Foundation (DFG), Excellence Initiative by the German federal and state governments to promote top-level research at German universities (Grant no. F-003661-553-41A-1132104).

References

[1] S. Milles, M. Soldera, T. Kuntze, and A. F. Lasagni: Appl. Surf. Sci., 525, (2020) 146518.
[2] C. Zwahr, D. Günther, T. Brinkmann, N. Gulow, S. Oswald, M. G. Holthaus, and A. F. Lasagni: Adv. Healthc. Mater., 6, (2017) 1600858.
[3] D. Y. You, X. D. Gao, and S. Katayama: Sci. Technol. Weld. Joi., 19, (2014) 181.
[4] A. Wetzig, P. Herwig, J. Hauptmann, R. Baumann, P. Rauscher, M. Schlosser, T. Pinder, and C. Leyens: Procedia Manufacturing, 29, (2019) 369.
[5] S. H. van der Poel, M. Mezera, G. R. B. E. Römer, E. G. de Vries, and D. T. A. Matthews: Lubricants, 7, (2019) 8.
[6] Andrés F. Lasagni: Industrial Photonics, 3 (2016) 32.
[7] T. Tavera, N. Pérez, A. Rodríguez, P. Yurrita, S. M. Olaizola, and E. Castaño: Appl. Surf. Sci., 258, (2011) 1175.
[8] V. Lang, A. Rank, and A. F. Lasagni: Adv. Eng. Mater., 19, (2017) 1700126.
[9] A. Madelung, S. Alamri, T. Steege, B. Krupop, A. F. Lasagni, and T. Kunze: Adv. Eng. Mater., 32 (2021) 2001414.
[10] D. Fabris, A. F. Lasagni, M. C. Fredel, and B. Henriques: Ceramics, 2, (2019) 578.
[11] M. Soldera, S. Alamri, P. A. Sürmann, T. Kunze, and A. F. Lasagni: Nanomaterials, 11, (2021) 129.
[12] S. Alamri and A. F. Lasagni: Proc. SPIE, Vol. 10092, (2017) 1009219.
[13] C. Gachot, A. Rosenkranz, S. M. Hsu, and H. L. Costa: Wear, 21, (2017) 372.
[14] T. Purtonen, A. Kalliosaari, and A. Salminen: Physics Procedia, 56, (2014) 1218.
[15] J. Luo, Y. Liang, and G. Yang: Rev. Sci. Instrum., 83, (2012) 053102.
[16] E. V. Bordatchev and S. K. Nikumb: Meas. Sci. Technol., 13, (2002) 836.
[17] V. Schulze and P. Weber: Proc. ICALEO 2011, (2011) 966.
[18] T. Steege, S. Alamri, A. F. Lasagni, and T. Kunze: Sci. Rep., 11, (2021) 14540.
[19] X. Zhang, Y. Chen, and J. Hu: Prog. Aerosp. Sci., 97, (2018) 22.
[20] M. A. Hamstad and A. K. Mukherjee: United States: N. p. (1978) 6858214.
[21] B.-A. Behrens, A. Bouguecha, C. Buse, K. Wölki, and A. Santangelo: Arch. Civ. Mech. Eng., 16, (2016) 724.
[22] B.-A. Behrens, S. Hübner, and K. Wölki: J. Manuf. Process., 29, (2017) 281.
[23] F. Bai, D. Gagar, P. Foote, and Y. Zhao: Mech. Syst. Signal. PR., 84, (2017) 717.
[24] J. W. Cooley and J. W. Tukey: Math. Comp., 19, (1965) 297.
[25] S. Palanco and J. Laserna: Appl. Opt., 42, (2003) 6078.
[26] P. Bournot, P. A. Pincosy, G. Inglesakis, M. Autric, D. Dufresne, and J.-P. Caressa: Gasd. Exp. Sys., (1980) 257.
[27] T. Steege, F. Schell, A. Belkin, and A. F. Lasagni: Proc. SPIE, Vol. 11988, (2022) 1198807.
[28] D. B. Brayton: Appl. Opt., 13, (1974) 2346.

[29] M. Bieda, A. F. Lasagni, and E. Beyer: Proc. OPTICS, 132 (2010) 900.

[30] E. Brochu, V. M. Cora, and N. de Freitas: CoRR, 1012 (2010), 2599.

(Received: July 8, 2023, Accepted: December 22, 2023)